THE JOURNAL OF BIOLOGICAL CHEMISTRY VOL. 285, NO. 45, pp. 34746–34756, November 5, 2010
Printed in the U.S.A.

Mating Pheromone in *Cryptococcus neoformans* Is Regulated by a Transcriptional/Degradative "Futile" Cycle*[S]

Received for publication, April 21, 2010, and in revised form, August 12, 2010 Published, JBC Papers in Press, August 27, 2010, DOI 10.1074/jbc.M110.136812

Yoon-Dong Park[‡], John Panepinto[§], Soowan Shin[¶], Peter Larsen[‖], Steven Giles[**], and Peter R. Williamson[‡¶1]

*From the [‡]Laboratory of Clinical Infectious Diseases, NIAID, National Institutes of Health, Bethesda, Maryland 20892, the [§]Department of Microbiology and Immunology, Witebsky Center for Microbial Pathogenesis and Immunology, University of Buffalo, Buffalo, New York 14214, the [¶]Section of Infectious Diseases, Department of Medicine, University of Illinois, Chicago, Illinois 60612, the [‖]Biosciences Division, Argonne National Laboratory, Lemont, Illinois 60439, and the **Department of Bacteriology, University of Wisconsin, Madison, Wisconsin 53701*

Sexual reproduction in fungi requires induction of signaling pheromones within environments that are conducive to mating. The fungus *Cryptococcus neoformans* is currently the fourth greatest cause of infectious death in regions of Africa and undergoes mating in phytonutrient-rich environments to create spores with infectious potential. Here we show that under conditions where sexual development is inhibited, a ~17-fold excess of *MFα* pheromone transcript is synthesized and then degraded by a DEAD box protein, Vad1, resulting in low steady state transcript levels. Transfer to mating medium or deletion of the *VAD1* gene resulted in high level accumulation of *MFα* transcripts and enhanced mating, acting in concert with the mating-related *HOG1* pathway. We then investigated whether the high metabolic cost of this apparently futile transcriptional cycle could be justified by a more rapid induction of mating. Maintenance of Vad1 activity on inductive mating medium by constitutive expression resulted in repressed levels of *MFα* that did not prevent but rather prolonged the time to successful mating from 5–6 h to 15 h ($p < 0.0001$). In sum, these data suggest that *VAD1* negatively regulates the sexual cell cycle via degradation of constitutive high levels of *MFα* transcripts in a synthetic/degradative cycle, providing a mechanism of mRNA induction for time-critical cellular events, such as mating induction.

To initiate sexual development, fungi produce signaling pheromones to indicate their presence and their mating compatibility. Within their natural environment on environmental surfaces, successful mating requires a close physical association that is easily disturbed for non-motile organisms, such as yeast, suggesting that rapid induction might improve the chances for successful reproduction. Induction of mating requires pheromone production and has been most extensively studied in the model ascomycete, *Saccharomyces cerevisiae*, where the production of mating factor precursors is followed by post-translational modifications to yield active pheromones. Local proximity of compatible yeast cells results in pheromone binding to a cognate heterotrimeric G-protein-coupled receptor on cells of the opposite mating type, followed by activation of a mitogen-activated protein kinase (MAPK) cascade that leads to cell cycle arrest followed by cell fusion and ascospore development (1). After cell fusion, compatibility of the two mating partners is confirmed intracellularly by two MAT-encoded regulatory transcription factors; in ascomycota, the MAT locus encodes transcription factors of one of three types, homeodomain proteins, α-box, or high mobility group proteins (2).

Cryptococcus neoformans is a yeastlike basidiomycete human pathogen that undergoes a dimorphic transition to hyphal filamentous growth during the sexual cycle, which, in the environment, robustly occurs in a specialized niche of pigeon guano (3) as well as on plant surfaces (4). Stimulated by plant phytochemicals, sexual reproduction is believed to be important to the initiation of infections by virtue of the production of infectious spores (4–6). Indeed, human infections have been described after inhalation of infectious particles from environments such as soil contaminated with pigeon excreta (7). The implication of sexual development for virulence and infectivity is particularly important because the fungus causes a highly lethal meningoencephalitis in both immunocompetent and immunocompromised persons and has caused a virtual explosion in HIV-related cases within regions of Africa and Asia. Indeed, cryptococcosis has now become the fourth leading cause of death in sub-Saharan Africa, outpacing other well known infections, such as tuberculosis (8). Although the fungus is normally haploid during most growth conditions, including infection, under appropriate conditions and in response to mating pheromones, the two mating partners (α and **a**) produce conjugation tubes, and the cells fuse (9–12). Controlling and propagating sexual development is a large mating type locus of greater than 100 kb (1, 13, 14). The MAT locus contains ~25 genes and includes pheromone and homeodomain genes as well as those involved in the pheromone-responsive MAPK cascade, meiosis, and sporulation. In the principal infectious species of *C. neoformans*, serotype A, the number of pheromone genes varies between the two stable mating types. The **a** alleles contain three unlinked 130-bp *MF**a*** pheromone genes embedded in 900–5,000-bp amplicons identical within an allele but not between species. In contrast, the α alleles contain four *MFα* pheromone genes embedded in ~500-bp conserved repeats (14, 15). Expression studies of mating pheromones dur-

* This work was supported, in whole or in part, by National Institutes of Health Grants AI45995 and AI49371 and by the Intramural Research Program of the National Institutes of Health, NIAID. This work was also supported by American Heart Association Grant 0725736Z.

[S] The on-line version of this article (available at http://www.jbc.org) contains supplemental Tables S1–S3 and Figs. S1–S6.

[1] To whom correspondence should be addressed: 9000 Rockville Pike, Bldg. 10, Rm. 11N234, MSC 1888, Bethesda, MD 20892. Fax: 301-480-7321; E-mail: williamsonpr@mail.nih.gov.

ing infection of mice as well as knock-out experiments have confirmed that intact expression of this signaling peptide is required for wild-type levels of virulence (16). Two major signaling pathways, the pheromone-responsive Cpk1 mitogen-activated protein kinase (MAPK) pathway and the cyclic AMP (cAMP) pathway, have been shown to modulate both differentiation (during mating or monokaryotic fruiting) and the production of two principal virulence factors, capsule and laccase (17). A MAPK signaling cascade has also been defined that functions in sensing pheromones during mating (17, 18). In addition, a unique Hog1 regulatory pattern was observed in a serotype A *C. neoformans* strain. Serotype A Δ*hog1* mutants were found to be attenuated in virulence via the MAPK cascade, and mating competence was increased, showing the importance of this regulatory pathway and the interrelationship between mating and virulence in this fungal pathogen (19).

Previously, we demonstrated that Vad1 (virulence-associated DEAD box protein), having structural homology to the RCK/p54 family of DEAD box proteins, is an important regulator of virulence in *C. neoformans* (20). RCK/p54 family members have an interesting mechanism of transcriptional regulation in that they act to recruit mRNA transcripts to cytoplasmic P-bodies for degradation via a *CCR4*-dependent mechanism of decapping and deadenylation followed by 3′–5′ degradation (21). In the present study, RNA immunoprecipitation of an epitope-tagged Vad1 followed by microarray identified *MFα* transcripts as direct targets within a set of *C. neoformans* genes. Interestingly, we found that the mating pheromone, *MFα*, is simultaneously synthesized and degraded at high rates under vegetative growth conditions, resulting in the low, repressed levels of transcript reported previously (19). Transfer to an environmentally relevant pigeon guano mating medium resulted in no change in *MFα* transcript synthesis but rather stabilization of the mRNA degradative process, resulting in prompt induction of steady state levels of *MFα*, accompanied by mating induction. These studies suggest that vegetative growth in yeast is accompanied by the maintenance of an apparent "futile" cycle of pheromone transcriptional synthesis and degradation, facilitating a mechanism for prompt induction of time-critical phenotypes, such as sexual development.

EXPERIMENTAL PROCEDURES

Strains and Media—All experiments were conducted in a genetic background of *C. neoformans* strain serotype A H99 (ATCC 208821). A complete list used in this study is described in supplemental Table S1. *Escherichia coli* DH10B (Invitrogen) was the host strain for recovery and amplification of plasmids. The fungal strains were grown in YPD medium (2% glucose, 1% yeast extract, 2% Bacto-peptone) or YPD agar medium (YPD and 2% agar). Asparagine minimum selective medium for transformant selection and for detection of laccase production was previously described (22). V8 juice and pigeon guano medium were used for mating assays as described (3, 23).

DNA and RNA Preparation and Blotting—Primers used in this study are described in supplemental Table S3. DNA extraction was conducted according to the protocol of Casadevall and Perfect (7). RNA was isolated, and Northern blots were performed as described previously (20). DNA probes were labeled with [α-^{32}P]ATP for both Southern and Northern blots using the RadPrime DNA Labeling System (Invitrogen) according to the manufacturer's protocol. Transcript levels of the *MFα* pheromone genes were monitored by Northern blot analysis hybridized with a PCR-amplified fragment of either the conserved *MFα* ORF to measure total pheromone transcripts using primers MFα1-ORF-S1 and MFα1-ORF-A or a non-conserved 3′-UTR fragment to distinguish the pheromone genes using primers for *MFα1* (MFα1–3′-UTR-NS and MFα1–3′-UTR-NA) and for *MFα2,3,4* (MFα2–3′-UTR-NS and MFα2–3′-UTR-NA). RNA stability was measured for the indicated strains by time course experimentation by Northern blot analysis or real-time PCR of total RNA from mid-log phase cells harvested at 0, 10, 20, 30, and 60 min following the addition of a 500 μg/ml concentration of the transcription initiation inhibitor 1,10-phenanthroline as described (24).

Construction of a c-myc-VAD1- and GPD-GFP-expressing Cryptococcal Strain—To construct a c-*myc*-Vad1 fusion protein expression plasmid, a 2.4-kb genomic fragment encompassing the full ORF of *VAD1* plus c-*myc* at both the N and C termini of *VAD1* was PCR-amplified using a primer set of *myc*-VAD1-S and *myc*-VAD1-A. After digestion with MunI, the fragment was cloned into a cryptococcal expression vector, pORA-KUTAP, containing the *EF1-α* terminator under the control of a cryptococcal actin promoter (25), and introduced into Δ*vad1*-FOA mutant cells (YP510) by electroporation as described previously (26), and transformants were selected on uracil-containing asparagine minimum-selective medium agar plates. For *GPD-GFP* constructs (strains YP104, YP108, YP111, YP114, YP119, and YP126), the indicated 5′-UTR and/or 3′-UTR of the *MFα1* gene was PCR-amplified using primers described in supplemental Table S2 and cloned into pORA-KUTAP. The *HOG1* overexpression construct (strain YP127) was produced by PCR amplification of the *HOG1* ORF using primer set HOG1-S and HOG1-A, followed by digestion and ligation into a compatible site of pORA-KUTAP vector.

RNA Immunoprecipitation and Microarray Analysis—Because these are the first studies using this approach in *C. neoformans*, RNA immunoprecipitation was performed by an adaptation using a method previously described for *Saccharomyces* (27). Briefly, protein G-Sepharose (Sigma) was washed three times with 50 mM Tris-HCl (pH 8.0), 150 mM NaCl, 0.1% Nonidet P-40, and 30 μg of anti-*myc* monoclonal antibodies (Sigma) was added and incubated for 1 h at 4 °C. The Sepharose-bound mAb was washed five times in the same buffer at 4 °C. For immunoprecipitation, c-*myc*-Vad1 cells were grown to mid-log phase in YPD at 30 °C. Cells were harvested by centrifugation, and the cells were washed twice in 25 mM Hepes-KOH (pH 7.5), 150 mM KCl, 2 mM $MgCl_2$. Cells were resuspended in the above buffer containing 20 mM vanadyl ribonucleoside complexes (Sigma), 200 units/ml RNaseOUT (Sigma), 0.1% Nonidet P-40, 1 mM DTT with protease inhibitor mixture. Glass beads were added, and the samples were vortexed for 1 min. The supernatants were removed and centrifuged for 10 min at 3,000 × g_{max}. Extracts were incubated with anti-*myc* antibodies coupled to protein G-Sepharose for 1 h at 4 °C. Beads were washed seven times in 25 mM Hepes-KOH (pH

7.5), 150 mM KCl, 2 mM $MgCl_2$ and were eluted in 50 mM Tris·HCl (pH 8.0), 100 mM NaCl, 10 mM EDTA, 1% SDS for 10 min at 65 °C. A portion of each eluate was extracted with phenol/chloroform and ethanol-precipitated to isolate RNA. RNA from Vad1 *myc*-tagged and -untagged control total RNA were fluorescently labeled with Cy5 and Cy3 dyes, respectively, and were analyzed by simultaneous hybridization to *C. neoformans* microarrays (28).

Microarray slides were scanned on a GSI Lumonics ScanArray Lite. Microarray data were acquired with Packard Bioscience QuantArray 3.0. For microarray data analysis, feature signal (RNA from c-*myc*-Vad1-expressing cells) was corrected for local background, and the corrected signal was expressed as a function of the number of standard deviations of each signal above a global signal average of the whole array,

$$Corrected\_Signal = Raw\_Signal - (\mathrm{Ave}(All\_Signal)/\mathrm{S.D.}(All\_Signal)) \quad \text{(Eq. 1)}$$

where *Signal* is equal to the background corrected signal intensity, Ave(*All_Signal*) is the average of all background corrected signals on the array, and S.D.(*All_Signal*) is the standard deviation of all background corrected signals on the array. Significance of the signal was calculated as the two-tailed *p* value of a *z*-test for all replicate features, using the S.D. value of all measured features on the array. *p* values were corrected for false discovery rate using the Benjamini-Hochberg method (29).

Mating Assay—Haploid fruiting, confrontation, fusion competence, and filamentation assays were performed as described previously with slight modification (3, 30–32). Briefly, mating experiments were performed by coincubating cells of opposite mating type on V8 mating medium with or without glucose in the dark at room temperature for 2–7 days as indicated. For the confrontation assay, α cells were streaked in confrontation with **a** cells on V8 medium, followed by incubation for 1–3 weeks as indicated at room temperature in the dark. Images of mating and confrontation assays were captured with a Leica microscope equipped with a digital camera. To measure the fusion ability, equal numbers of strains YP548 (H99 + NAT) and YP549 (H99 + *VAD1* + NAT) were mixed with YP550 (KN99 + NEO) and incubated on duplicate plates of pigeon 25% guano medium for 0, 1, 2, 3, 4, 5, 6, 7, 8, 9, 13, and 15 h, and the mating colonies were harvested and spread on YPD medium containing nourseothricin (50 μg/ml) and G418 (100 μg/ml). Statistical comparison was made by a two-way analysis of variance with adjustment for multiple comparisons using GraphPad Prism 5.

Transcriptional Run-on Analysis—Transcriptional run-on was performed using methods described previously (33) with the following modifications. Cells were grown at 30 °C in YPD with agitation until the culture reached an A_{600} of 1.0. The cells were centrifuged for 5 min at 4,000 × *g* and resuspended in YPD and pigeon guano medium, following another culture for 30 min at 30 °C. Run-on analysis was performed in two independent experiments.

Fluorescent Microscopy—Filamentous hyphae were harvested from V8 medium, fixed in 70% ethanol, washed once with 1 ml of ice-cold PBS, resuspended in 100 μl of PBS, and stained with calcofluor white and propidium iodide according to the instructions of the manufacturer (Molecular Probes, MoBiTec, Göttingen, Germany). Cells were visualized by epifluorescence or bright field using an OLYMPUS IX70 microscope. For GFP expression, yeast cells from each of the three individual transformants were observed for epifluorescence, and relative intensity was measured using Slidebook 4.2 (digital microscopy software; Olympus).

Virulence Studies—Virulence studies were conducted using a previously described intravenous mouse meningoencephalitis model with 10 Swiss albino mice on cryptococcal strains expressing plasmids in equivalent copy number determined by uncut Southern analysis (34). Episomal expression of plasmids in *C. neoformans* have statistically insignificant differences in virulence from wild-type parental strains (35). Fungal viability was confirmed by growth of inocula on YPD agar. Animal studies were approved by the University of Illinois at Chicago Animal Care Committee. Statistical comparison was made by a log rank comparison using GraphPad Prism 5.

RESULTS

Identification of mRNAs Associated with the Vad1 Protein—Because *VAD1* contains putative RNA-binding domains as determined by sequence studies (20), we hypothesized that Vad1 may directly bind RNA transcripts as a method of regulation. Thus, we set out to characterize the mRNA binding profile of Vad1 by using RNA immunoprecipitation followed by microarray analysis. To identify mRNAs associated with the Vad1 protein, we expressed an N- and C-terminal double c-*myc*-tagged Vad1 fusion protein in a Δ*vad1* strain (supplemental Fig. S1*A*). Expression of c-*myc*-Vad1 was found to restore defective laccase expression previously reported in Δ*vad1* cells (20), indicating that the c-*myc*-fused Vad1 protein was functional (supplemental Fig. S1*B*). Immunoprecipitation of the c-*myc*-Vad1 from mid-log phase fungal cells with a c-*myc* monoclonal antibody followed by RNA purification, cDNA synthesis, and microarray hybridization identified 32 unique mRNA transcripts. Thirteen of these represented conserved proteins (see the Broad Institute Web site). These genes represent a broad array of metabolic processes, including ubiquinone biosynthesis, cell wall and mitochondrial function, and cell cycle regulation (Table 1). Three genes among these transcripts were further confirmed by RT-PCR (supplemental Fig. S2). Within this group, we found two sets of mating pheromone transcripts within the most highly enriched RNAs. These data suggest that *VAD1* regulates multiple transcripts, including *MFα1*, by RNA binding.

Role of VAD1 in Maintenance of Steady State Levels of MFα Transcripts—Because the *MFα* pheromone is a well characterized gene in *C. neoformans* (12, 36) and has an established role in virulence and mating (37), we decided to model mechanistic studies of *VAD1* using *MFα* expression. There are four mating pheromone genes in the serotype A *C. neoformans* strain H99 (Fig. 1*A*) (15). *MFα2*, *-3*, and *-4* are identical, having the same coding as well as 5′- and 3′-UTRs. Two nucleotides within the single coding region differ between *MFα1* and the other mating pheromones but encode the same amino acids. In addition, the 3′-UTRs differ substantially between *MFα1* and the other three

TABLE 1

Conserved genes showing Vad1 binding by RNA Immunoprecipitation

A partial list of target genes after deletion of hypothetical genes is given. A complete list is provided in supplemental Table S2.

Locus	Name	GO terms (function, process, component)	S.D. above[a]	*p* value[b]
CND05750	Pheromone α		18.4	0
CNE00990	Ubiquinone biosynthesis-related protein putative	Ubiquinone biosynthetic process (GO term accession no. 6744), mitochondrion (5739)	16.7	0
CND05690	MFα3		12.2	0
CNF03500	Cell wall organization and biogenesis-related protein putative	Cell wall organization (7047), cytoplasm (5737), nucleus (5634)	12.0	0
CND00920	Mitochondrion protein putative	Mitochondrion (5739)	9.9	0
CND03890	Asparagine-tRNA ligase putative	Asparagine-tRNA ligase activity (4816), translation (6412), mitochondrion (5739)	8.1	0
CNA05980	Cytoplasm protein putative	Cytoplasm (5737)	7.8	4.108E-15
CNE04100	Cyclin-dependent protein kinase regulator putative	Cyclin-dependent protein kinase regulator activity (16538), general RNA polymerase II transcription factor activity (16251), meiosis (7126), negative regulation of transcription from RNA polymerase II promoter (122), transcription factor complex (5667)	6.3	1.243E-10
CNA05980	Cytoplasm protein putative	Cytoplasm (5737)	6.3	1.254E-10
CNN02220	Epoxide hydrolase 1 (EC 3.3.2.3) putative		6.1	4.843E-10
CNI01880	ATP-dependent RNA helicase putative	RNA helicase activity (3724), mRNA export from nucleus (6406), cytoplasm (5737), nuclear pore (5643)	5.2	8.812E-08
CNF04720	Pim1 protein (poly(a)+ RNA transport protein 2) putative	Signal transducer activity (4871), rRNA export from nucleus (6407), ribosome export from nucleus (54), nucleus (5634)	4.0	3.442E-05
CNL05600	Pyruvate dehydrogenase e1 component β subunit mitochondrial precursor (EC 1.2.4.1) putative	Pyruvate dehydrogenase (acetyl-transferring) activity (4739), pyruvate metabolic process (6090), mitochondrial pyruvate dehydrogenase complex (5967), mitochondrion (5739)	3.7	9.499E-05

[a] S.D. above indicates the number of S.D. values (based on four microarray analyses) that the indicated gene signal was above the background signal, the latter defined as the mean level of signal of all genes in the immunoprecipitated RNA sample.

[b] *p* values were corrected for false discovery rate using the Benjamini-Hochberg method.

mating pheromones. Thus, to distinguish *MFα1* from *MFα2*, *-3*, and *-4*, Southern blot analysis was performed with 3′-UTR-specific probes, including 200 bp of each of the *MFα* gene groupings (supplemental Fig. S3). These probes were then used to determine steady state levels of *MFα* transcripts from either wild type or a *C. neoformans* Δ*vad1* strain. As shown in Fig. 1, *B* and *C*, the Δ*vad1* mutant showed accumulation of *MFα* transcripts by Northern blot compared with wild type from either mid-log cells (*Glu* (+)) or from cells incubated under starvation conditions (*Glu* (−)). This was observed using either an *MFα* ORF probe that measures total *MFα* transcription (Fig. 1*B*) or a 3′-UTR sequence that distinguishes *MFα1* from transcripts *MFα2*, *-3*, and *-4* (Fig. 1*C*). Vad1-dependent *MFα* accumulation was also observed in the presence of an opposite mating partner shown previously to potentiate *MFα1* transcription (data not shown) (19). Neither mid-log phase wild-type cells nor wild-type cells incubated under starvation medium exhibited hyphal development after incubation with an appropriate **a** mating partner (data not shown). Taken together, these data suggest that *VAD1* negatively regulates mating by repression of the mating pheromone, *MFα*.

Vad1 Affects Stability of MFα mRNA—Based on the structural homology of *VAD1* to RCK/p54 family protein genes involved in mRNA degradation (38), we hypothesized that *VAD1* also acts by facilitating degradation of target transcripts. Thus, we assessed for *VAD1*-dependent degradation of *MFα* transcripts after mRNA synthesis was inhibited by 1,10-phenanthroline as described previously (39). As shown in Fig. 1*D*, *MFα* mRNA from mid-log phase fungal cells exhibited time-dependent degradation with a half-life of 10 ± 1 min, whereas the Δ*vad1* mutant strain showed stabilization of the *MFα* stable transcript with a half-life of 60 ± 20 min (±S.E.; $p < 0.05$), respectively. Thus, accumulation of steady state levels of *MFα* in Fig. 1, *B* and *C*, is most likely the result of *VAD1*-dependent degradation of the *MFα* target transcript. This *VAD1*-dependent degradation was also observed using probes specific for *MFα1* or *MFα2,3,4* (data not shown).

Because mRNA decapping represents a critical step in mRNA turnover mediated by RCK/p54 members (40), we tested whether Vad1-dependent degradation is mediated by decapping of *MFα1*. The presence of capped *MFα1* transcripts was assayed by PCR amplification of a cDNA product obtained after sequential ligation of a 5′ RNA adapter following treatment with tobacco acid pyrophosphatase by a method previously described (41) (supplemental Fig. S4). Using this method, abundant capped transcripts were detected in both WT and Δ*vad1* mutants, whereas 30 min after inhibition of transcript synthesis, the Δ*vad1* mutant demonstrated greater accumulation of capped transcripts. This result supports a role for *VAD1* in transcript decapping, similar to other RCK/p54 members.

Both 5′- and 3′-UTRs Are Required for Vad1-dependent mRNA Degradation—To determine the role of the *MFα1* 5′-UTR and 3′-UTR in *VAD1*-dependent transcriptional degradation, we expressed a synthetic *MFα1* transcript containing green fluorescent protein sequence (GFP) to allow selective determination of transcript levels. The decay rates of *MFα1-GFP* in the wild-type (YP538) or transformed Δ*vad1* strains (YP539) were then compared after inhibition of transcription initiation by 1,10-phenanthroline. As shown in Fig. 2*A*, *MFα1-GFP* mRNA in wild-type cells decayed with a half-life of 6.9 ± 1.4 min, whereas in the Δ*vad1* strain, the half-life was increased to 18.2 ± 5.4 min (±S.E.; $p < 0.05$). This pattern is similar in

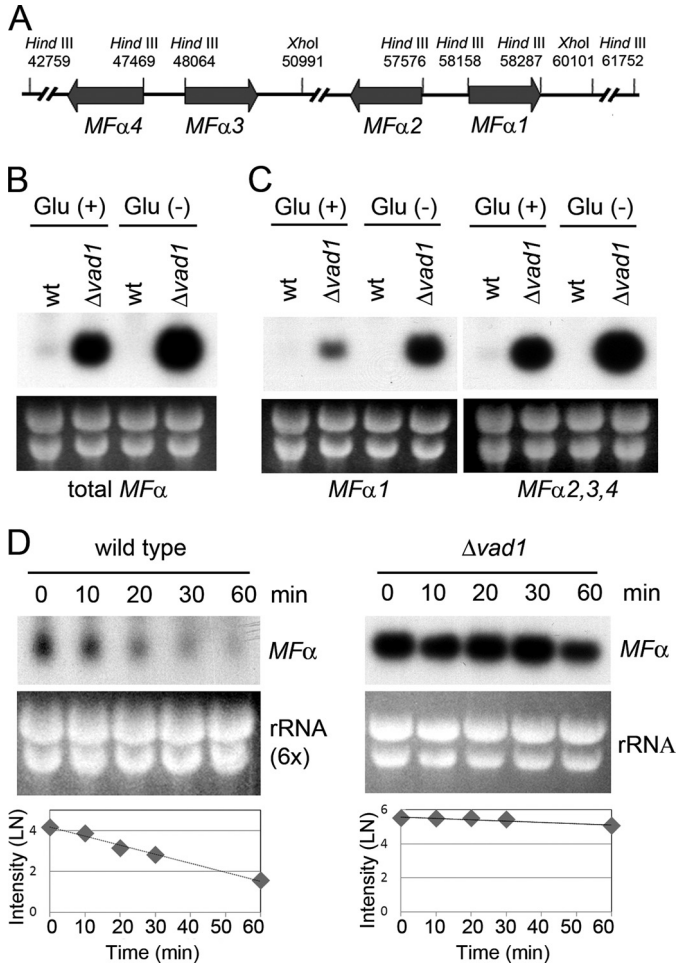

FIGURE 1. **Mutation of the *VAD1* gene increases steady state mating pheromone transcript levels by altering transcript degradation.** *A*, scheme of mating α locus of *C. neoformans* serotype A. The positions of restriction enzyme sites are indicated by *position numbers* of the MATα locus (14). *B*, Northern blot analysis was performed with total RNA isolated from wild type or Δ*vad1* strains grown to mid-log phase (*Glu* (+)) or after transfer to asparagine salts without glucose for 3 h (*Glu* (−)). The blot was hybridized with *MFα* ORF sequences to measure total *MFα* (*B*) or with a unique 3′-UTR sequence from the respective *MFα* genes (*C*). *D*, total RNA from wild type loaded at 6 times that of the Δ*vad1* mutant cells. The blot was hybridized with an ORF region from *MFα* genes (at the indicated times after transcriptional repression by 1,10-phenanthroline). The *graphs* demonstrate relative quantitative measurement of transcript levels of *MFα* normalized to the rRNA loading control by ImageQuant version 5.2 (Molecular Dynamics).

magnitude to rates of decay of native *MFα* as shown in Fig. 1*D*, although the increase in degradation in both strains may be due to instability introduced by the synthetic *GFP* sequence.

Next, we tested whether Vad1-dependent degradation is mediated by the presence of the 5′-UTR of *MFα1*, because many RNA-binding proteins mediate their effects by selective binding to a target motif in the 5′-UTR (42–44). As shown in Fig. 2*B*, time-dependent transcriptional levels of *GFP-MFα1*Δ5′-UTR expressed in a wild-type strain (YP532) were found to be stabilized, equal to that of a Δ*vad1* strain (YP533) transformed with an equivalent construct (YP532, $t_{½} = 40.1 \pm 4.5$; YP533, 43.7 ± 4.6 min ($\pm$S.E.; $p < 0.05$ *versus* WT in each case)), suggesting a role for the *MFα1* 5′-UTR in *VAD1*-dependent degradation.

In addition, we examined the role of the 3′-UTR by a replacement approach. Finding a role for *MFα1* 3′-UTR would suggest a function in RNA stability affecting processes such as deadenylation, which is dependent on the 3′-UTR (45). To test these possibilities, we expressed *MFα1-GFP*, replacing the *MFα1* 3′-UTR with an unrelated *EF1-α* 3′-UTR, which has been successfully used to express proteins in *C. neoformans* (25). As shown in Fig. 2*C*, replacement of the *MFα1* 3′-UTR (MFα1Δ3′-UTR-a) also resulted in stabilization of the *MFα* transcript, which was also evident using a equivalent construct containing a truncated 5′-UTR region (MFα1Δ3′-UTR-b) ($t_{½} > 60$ min $\pm$ S.E.; $p < 0.05$). Furthermore, to verify that transcription stabilization was not due to the GPD promoter or GFP sequence, we expressed the *MFα1* ORF alone under control of an *ACT1* promoter containing either a native 3′-UTR or a construct with the unrelated *EF1-α* 3′-UTR (ACT1-MFα1Δ5′-UTR). As shown in Fig. 2*D*, the stability of both constructs was also increased using the *ACT1* promoter, suggesting that the 3′-UTR alone or the GPD promoter sequences were not responsible for the increased stability of the synthetic constructs having deletions of either the 3′- or 5′-UTRs ($t_{½} > 60$ min $\pm$ S.E.; $p < 0.05$ *versus* WT). The above experiments took advantage of a 10-fold higher expression level of the synthetic *MFα1* genes relative to wild type *MFα*, which allowed quantification of the synthetic gene by a simple Northern blot. However, to confirm the specificity of the analysis, degradation of the two constructs shown in Fig. 2*D* were quantified by real-time PCR using a sense primer within the *ACT1* promoter and an antisense primer within the *MFα1* ORF. As shown in Fig. 2*E*, this analysis also showed increased transcriptional stability of the synthetic construct containing the replaced 5′ and 3′ regions ($t_{½} > 60$ min $\pm$ S.E.; $p < 0.01$). Taken together, these results indicate that both 5′- and 3′-UTRs of *MFα1* are required for *VAD1*-dependent mRNA degradation.

Accumulation of an MFα1-GFP Fusion Protein in a Δ*vad1 Mutant Strain of C. neoformans*—To determine if accumulation of *MFα1* transcripts was accompanied by increased protein levels, an MFα1-GFP fusion protein was expressed in wild type (YP538) and Δ*vad1* (YP539) strains, and protein levels were assessed by quantitative epifluorescence. Previous studies showed that MFα1-GFP fusion proteins expressed in *C. neoformans* showed an accumulation of epifluorescence in the fungal cell periphery, and fluorescence correlated with mating activity (46). As shown in Fig. 3, expression of the MFα1-GFP fusion proteins at 24 h showed greater levels of accumulation in the Δ*vad1* mutant strain of *C. neoformans* compared with that of an identical construct expressed in wild type cells. Quantification of the epifluorescence signal from 50 cells (subtracting each from an equivalent strain transformed with empty vector alone) showed an 11-fold increased accumulation in the Δ*vad1* mutant strain (77.2 ± 6.7 fluorescent units) compared with a wild-type strain transformed with an equivalent construct in equivalent copy number (6.6 ± 6.7 fluorescent units ($\pm$S.E.; $p < 0.001$)). Although quantification using GFP could be affected by differences in rates of cell wall and membrane protein binding, the large levels of accumulation in the Δ*vad1* mutant suggest that accumulated steady state transcript levels in Fig. 2*A* are also reflected in increased rates of MFα protein production.

Vad1 Mutation Enhances Mating in C. neoformans—To assess for a functional relationship between *VAD1* and *MFα1*

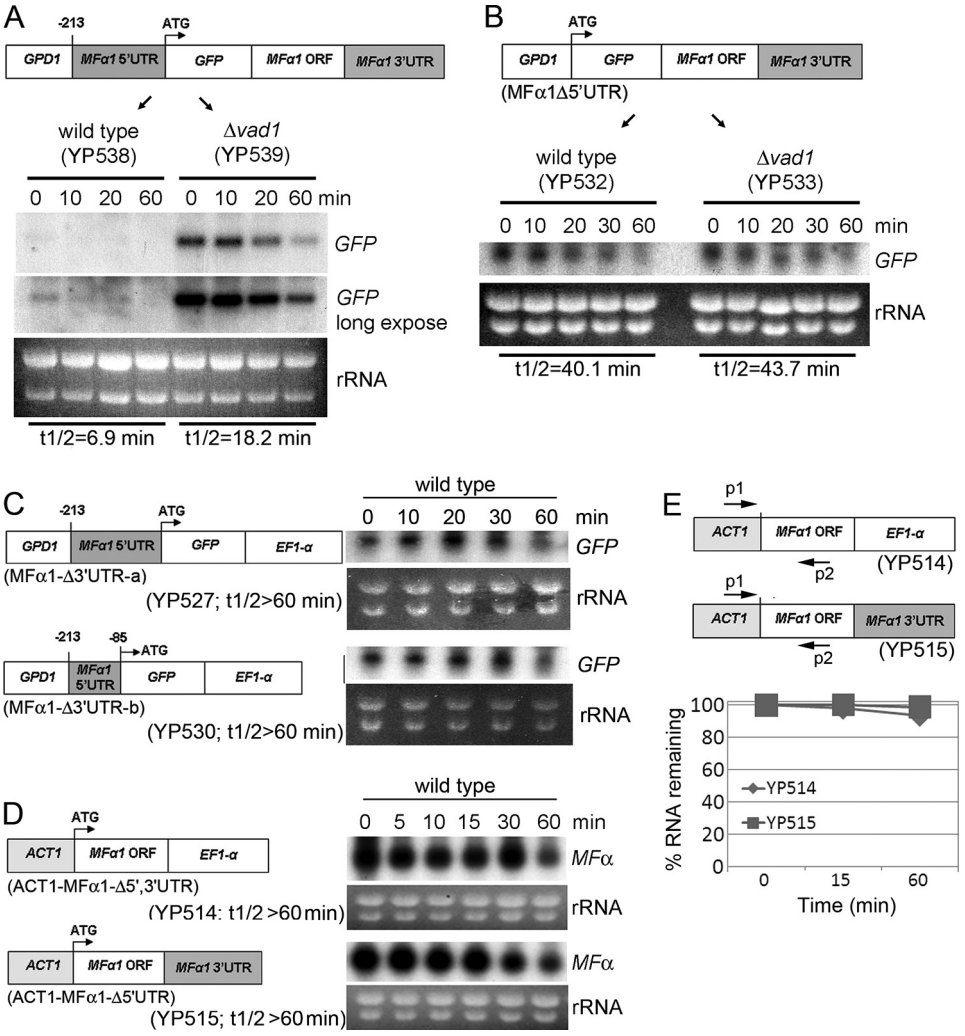

FIGURE 2. **Both 5′- and 3′-UTRs are required for mRNA degradation of *MFα1*.** Northern blot analysis was performed using total RNA isolated from the indicated strains at the indicated times after transcription repression by 1,10-phenanthroline. Each blot was hybridized with probes containing either *GFP* sequence or that of *MFα1*, as indicated. Schemes of the expressed synthetic genes are given in *A–D* and are described under "Experimental Procedures." *E*, real-time PCR was performed using a primer set of *ACT1* and MFα1-A, as described in the scheme, and using the same RNA as that used in Northern blot analysis from YP514 and YP515 at the 0, 10, and 60 min time points (Fig. 2*D*).

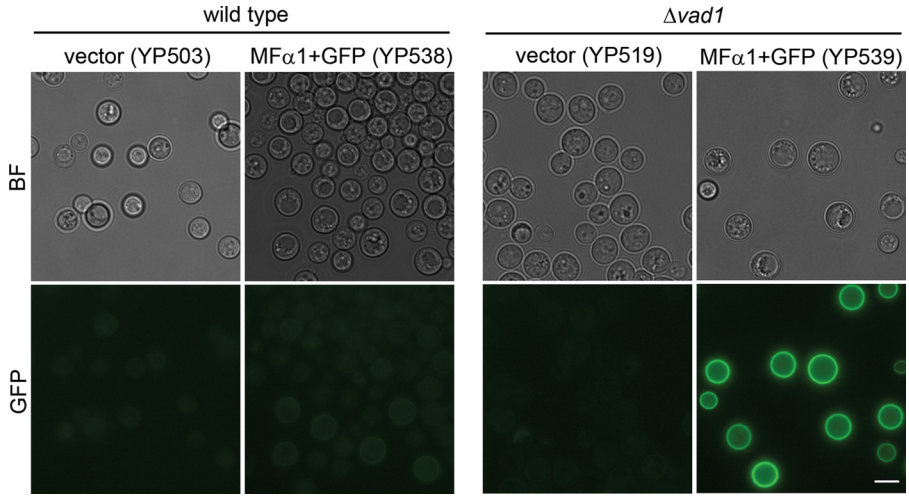

FIGURE 3. **Accumulation of an expressed MFα1-GFP fusion protein in a Δ*vad1* mutant strain.** Shown is microscopic localization of MFα1-GFP of the indicated strains in YPD medium. *BF*, bright field. *Bar*, 5 μm.

transcript levels, sexual cycle-related phenotypes of the Δ*vad1* mutant were compared with that of wild type under conditions described previously (19). Consistent with increases in mating pheromone, the Δ*vad1* mutant strain produced more abundant filaments than the wild type strain when incubated with *MAT***a** cells on mating medium either in the presence of glucose or without glucose conditions for 7 days (Fig. 4*A*). In addition, filamentation was reduced to wild type in a Δ*vad1* + *VAD1* reconstituted strain. To identify clamp junctions, we fixed and stained hyphae from the *MAT***a** × Δ*vad1* cross with calcofluor white and propidium iodide, which demonstrated two nuclei per filament cell and the presence of clamp junctions (Fig. 4*B*, *arrows*). Furthermore, in confrontation assays, Δ*vad1* was more effective in inducing pheromone-mediated conjugation tubes in its mating partner than wild type (Fig. 4*C*). However, incubation of the Δ*vad1* mutant on V8 medium did not result in observable haploid fruiting (data not shown). Taken together, these data suggest that deletion of the *VAD1* gene results in accumulation of *MFα* pheromone, which is functionally active and enhances mating-related structures in *C. neoformans*.

Similarly, overexpression of *MFα1* in wild-type strains using an *ACT1* promoter produced abundant filaments when incubated with *MAT***a** cells, showing that hyphae can be produced by increases in mating factor alone (Fig. 4*D*). Overexpression also resulted in a minimally elevated growth rate at 37 °C with the WT + *MFα* strain having a doubling time of 2.9 ± 0.1 h *versus* the WT plus empty vector strain having a doubling time of 3.2 ± 0.1 h (±S.E., $p = 0.1$). Despite this slight increase in growth rate, overexpression of *MFα1* resulted in a reduction in virulence using a mouse model. As shown in Fig. 4*E*, intravenous inoculation of *C. neoformans* strains overexpressing *MFα* resulted in attenuated virulence compared with

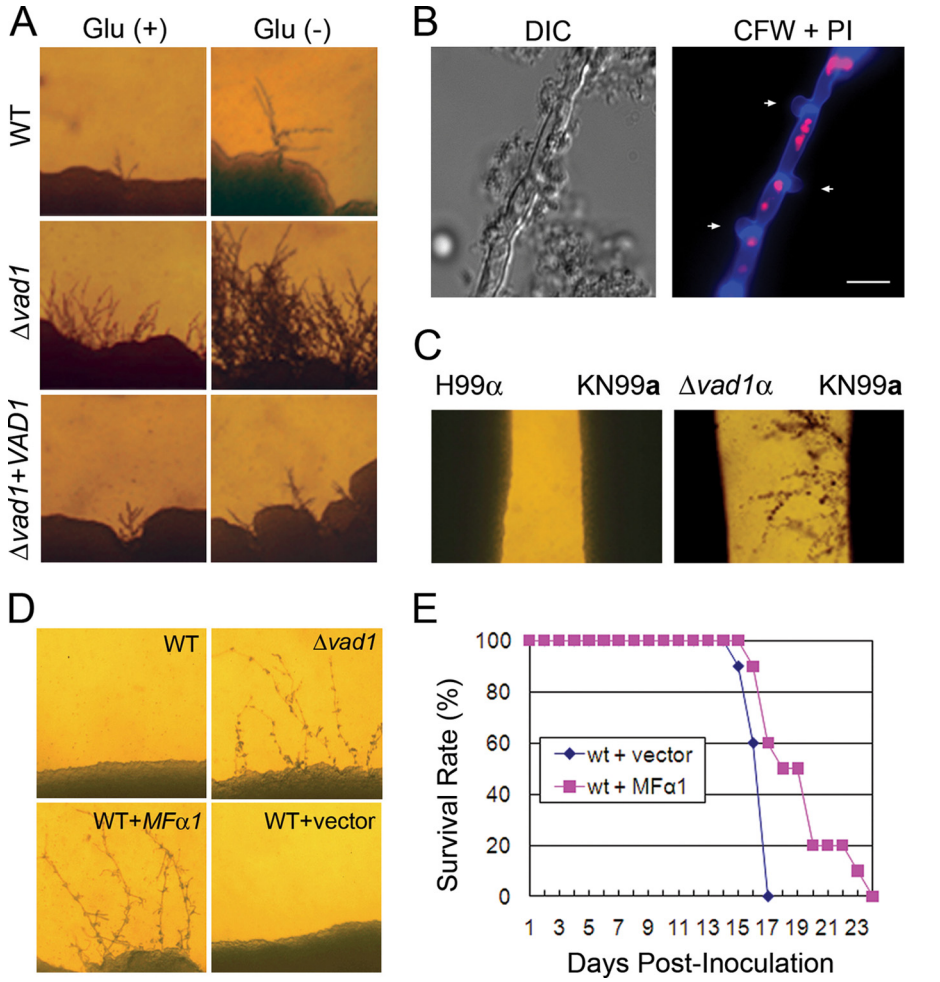

FIGURE 4. **Vad1 mutation enhances filamentation.** *MATα* wild type (H99) and Δ*vad1* strains were co-cultured (*A*) or confronted (*C*) with the *MAT***a** wild type (KN99) strain on V8 medium and incubated for 7 days at room temperature in the dark. Representative edges of the mating patches were photographed at ×40 magnification. *B*, filamentous hyphae from KN99XΔ*vad1* were fixed and stained with calcofluor white (*CFW*) and propidium iodide (*PI*), demonstrating clamp junctions (*arrows*), and DNA (*red*). *Bar*, 10 μm. *D*, the indicated strains were co-cultured with KN99 on V8 medium and incubated for 4 days at room temperature in the dark. *E*, analysis of virulence of *MFα* overexpressed in wild type strain compared with the wild type with empty vector alone using a mouse model of disseminated cryptococcosis with an intravenous inoculum of 1×10^5 yeast cells (10 mice/group; $p < 0.005$).

identical strains transformed with empty vector alone in identical copy number, consistent with previous data showing reduced virulence after *MFα* dysregulation created by *MFα* targeted deletion (12). These data suggest that excessive constitutive expression of mating pheromones in *C. neoformans* increases mating capacity but at a cost of reduced pathogenicity.

Mating Pheromone Transcripts Accumulate in Pigeon Guano Medium—Pigeon guano is a natural ecological niche of *C. neoformans* and is a potent inducer of mating by virtue of its rich source of phytometabolites (3). Thus, to assess for a physiological role of Vad1 in the regulation of mating, we studied *MFα* transcription after transfer from a rich medium (YPD) to a previously described mating medium made from pigeon guano (3). Interestingly, steady state levels of *MFα* in wild-type cells were highly induced at 30 min, whereas levels were high but not induced further in the Δ*vad1* strain (Fig. 5*A*). To determine relationships between *VAD1* and *MFα* stability in pigeon guano, we then assessed for *VAD1*-mediated degradation of *MFα* transcripts after a 30-min incubation on pigeon guano medium. As shown in Fig. 5*B*, *MFα* mRNA was found to persist in wild type cells in pigeon guano with a half-life of 17.9 ± 2.4 min, an increase over that found in YPD (10 ± 1 (±S.E.; $p < 0.04$)). However, overexpression of *VAD1* in wild-type cells resulted in rapid degradation of *MFα* even on pigeon guano to barely detectable levels. Similar to the effect on transcription, as shown in Fig. 5*C*, the relative intensities of MFα-GFP protein in wild-type cells showed a 4-fold increase after transfer to pigeon guano medium (from 6.6 ± 6.6 (YPD) to 26 ± 4.9 (pigeon guano) (±S.E.; $p < 005$)). Protein levels measured by GFP fluorescence were also highly enriched in Δ*vad1* cells but with no increase after transfer to pigeon guano medium (77.3 ± 6.7 *versus* 65.3 ± 10.5 (±S.E.; $p > 0.1$); Fig. 5*C*). In contrast, transcriptional run-on experiments demonstrated equivalent rates of *MFα1* transcript synthesis in rich medium or pigeon guano medium (Fig. 5*D*), despite the observed increase in steady state transcript levels (Fig. 5*A*). These data suggest that transfer to a physiological mating environment, simulated by pigeon guano medium, is accompanied by increases in steady state levels of *MFα*, mediated by a partial inhibition of *MFα* degradation.

If transfer to pigeon guano results in stabilization of synthesized *MFα* accompanied by an induction of mating, we reasoned that increasing *VAD1* gene dosing could affect mating efficiency. To assess for this, time course mating fusion experiments were conducted in which a H99 + empty vector + NAT (*MATα*) or an H99 + *VAD1* + NAT (*MATα*) *VAD1* overexpressor strain was crossed with a KN99 + NEO (*MAT***a**) strain and colonies were observed on double antibiotic-containing medium as described previously (30). Interestingly, overexpression of *VAD1* did not prevent mating (Fig. 5*E*, *left*), although *MFα* was reduced to levels associated with vegetative growth where mating does not occur. However, the time to successful mating measured by fusion assays was significantly delayed about 5–6 h in the *VAD1* overexpressor strain (Fig. 5*E* (*right*), $p < 0.0001$). This latter finding suggests that *VAD1*-mediated *MFα* induction plays a role in accelerating the time to efficient mating.

Relationship between VAD1 and Signal Transduction Pathway Genes—To assess for regulatory relationships between *MFα*, *VAD1*, and known signal transduction pathways, we per-

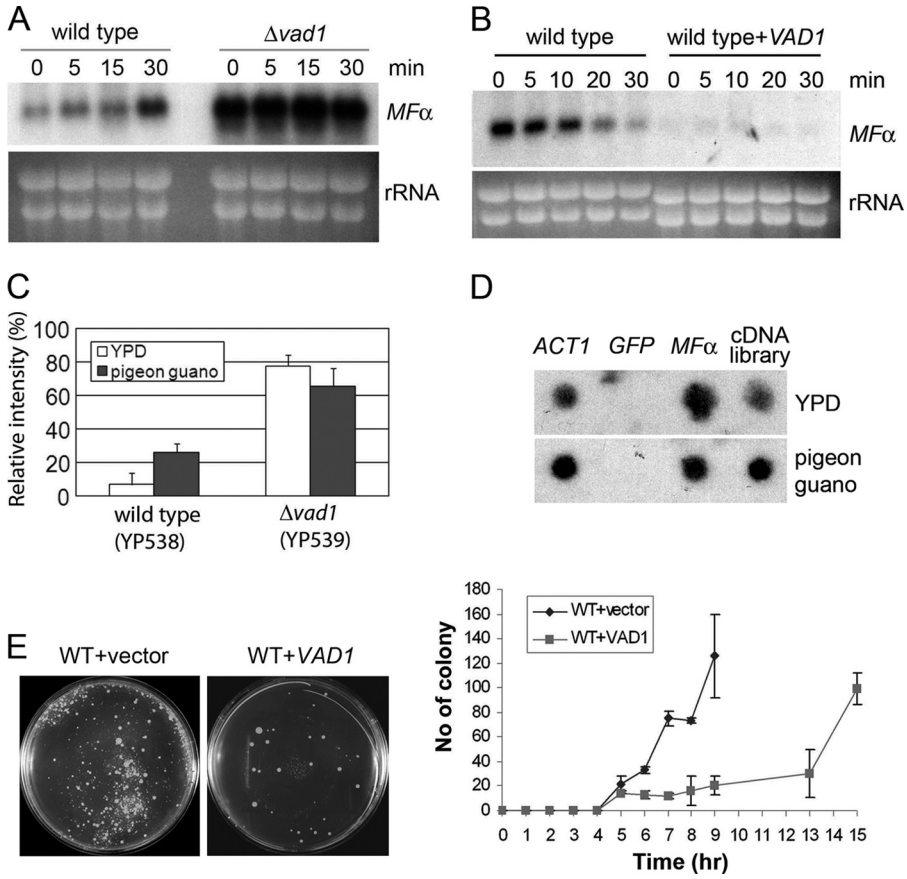

FIGURE 5. **Accumulation of both *MFα1* transcript and MFα1-GFP fusion protein on pigeon guano medium.** *A*, Northern blot analysis of steady state levels of *MFα1* of wild type and Δ*vad1* mutant cells upon transition to pigeon guano medium. RNA was prepared at the indicated times after transfer of cells from YPD to pigeon guano medium. Membranes were hybridized with *MFα* ORF sequences. *B*, wild type or *VAD1*-overexpressing strains (mid-exponential phase) were transferred to pigeon guano medium, and mRNA degradation was assayed. *C*, relative intensity of MFα1-GFP cultured on YPD or pigeon guano medium, measured by fluorescence microscopy as in Fig. 3*A*. *D*, transcriptional run-on analysis of *MFα1* in YPD and after a 30-min incubation on pigeon guano medium. *Dot blots* were prepared with PCR-amplified fragments (10 μg/sample) using primers from within the coding regions of the respective gene targets. *E*, fusion mating assays were performed as described under "Experimental Procedures." Agar plates were photographed at the indicated time points (*left*, 13 h), and fused colony numbers of indicated strains were counted and recorded (*right*). *Error bars*, S.E.

formed simultaneous Northern blot and filamentation analyses of cryptococcal mutants to identify genes whose mutants phenotypically mimic that of *VAD1*. This analysis compared mutants of *HOG1*, *STE12*, *PKA1*, and *GPA1*, previously associated with two *VAD1*-associated phenotypes, laccase and mating. Using hyphae formation as an indicator of sexual development, Δ*vad1* and Δ*hog1* mutant cells both exhibited robust production of hyphae when co-cultured with *MAT***a** wild type cells on V8 mating medium (supplemental Fig. S5*A*) as well as increased levels of *MFα* transcript (supplemental Fig. S5*B*), as reported previously for a Δ*hog1* strain (19). These data together suggest a common mating-associated phenotype linking the *VAD1-MFα1* and *HOG1-MFα1* pathways. Next, we investigated possible epistatic relationships between *VAD1* and *HOG1*. As shown in Fig. 6*A*, overexpression of *VAD1* in the Δ*hog1* strain reduced levels of the *MFα* transcript either in the presence or absence of a mating partner. This is to be expected because *VAD1* binding suggests a direct link between this regulator and the target transcript that would imply that *VAD1* acts downstream of *HOG1*. However, overexpression of *HOG1* in the Δ*vad1* mutant also reduced levels of *MFα* (Fig. 6*B*). In addition, *HOG1* overexpression could not restore wild-type degradation of *MFα* transcripts in Δ*vad1* mutant cells (supplemental Fig. S6), suggesting that *HOG1* acts through a parallel pathway. A direct action of *VAD1* on *HOG1* was felt to be less likely based on a failure to identify *HOG1* transcripts after immunoprecipitation of the Vad1 protein and failure to detect *HOG1* transcriptional changes after *VAD1* deletion (20). Similarly, both overexpression strains showed reduced filamentation from that of the respective parent Δ*hog1* or Δ*vad1* mutant strain (Fig. 6*C*), suggesting a phenotypic significance to the transcriptional epistatic studies. We were unable to test the phenotype of a double Δ*vad1*Δ*hog1* mutant because several crosses of a *vad1*α::*URA5* mutant strain and a *hog1***a**::*NEO* mutant strain yielded only single cross progeny in a PCR screen of 50 viable basidiospores. This suggests a synthetic lethality between the two genes, again more suggestive of a parallel pathway. However, as shown in Fig. 6*D*, the filamentation capacity of both mutant cells (Δ*vad1*xΔ*hog1*) was higher than that of single mutant cells (KN99xΔ*vad1* or H99xΔ*hog1*), which, again, could suggest independent pathways. As an independent corroboration of this hypothesis, degradation assays of the Δ*hog1* mutant demonstrated intact degradation of *MFα* in the absence of *HOG1* ($t_{½}$ = 7.2 ± 1.0 (±S.E.; $p < 0.05$ *versus* WT)), suggesting that *HOG1*-mediated derepression acts through a non-degradative pathway, such as transcriptional induction (Fig. 6*E*). Taken together, these data suggest an epistatic relationship in mating-related pathways whereby *HOG1* and *VAD1* regulate *MFα1* and hyphae formation via independent pathways.

DISCUSSION

In this study, we identified a set of 32 Vad1-binding transcripts, including those encoding the two sets of *MFα* pheromone genes, suggesting a role for Vad1 binding in degradation-specific regulation of transcription. Previous studies had implicated alternative substrate and mitochondrial processes as being dependent on *VAD1* (20), and many of the implicated transcripts (Table 1) encoded proteins traced to these gene ontology-linked processes. In both yeast and mammalian systems, numerous RNA-binding proteins have the

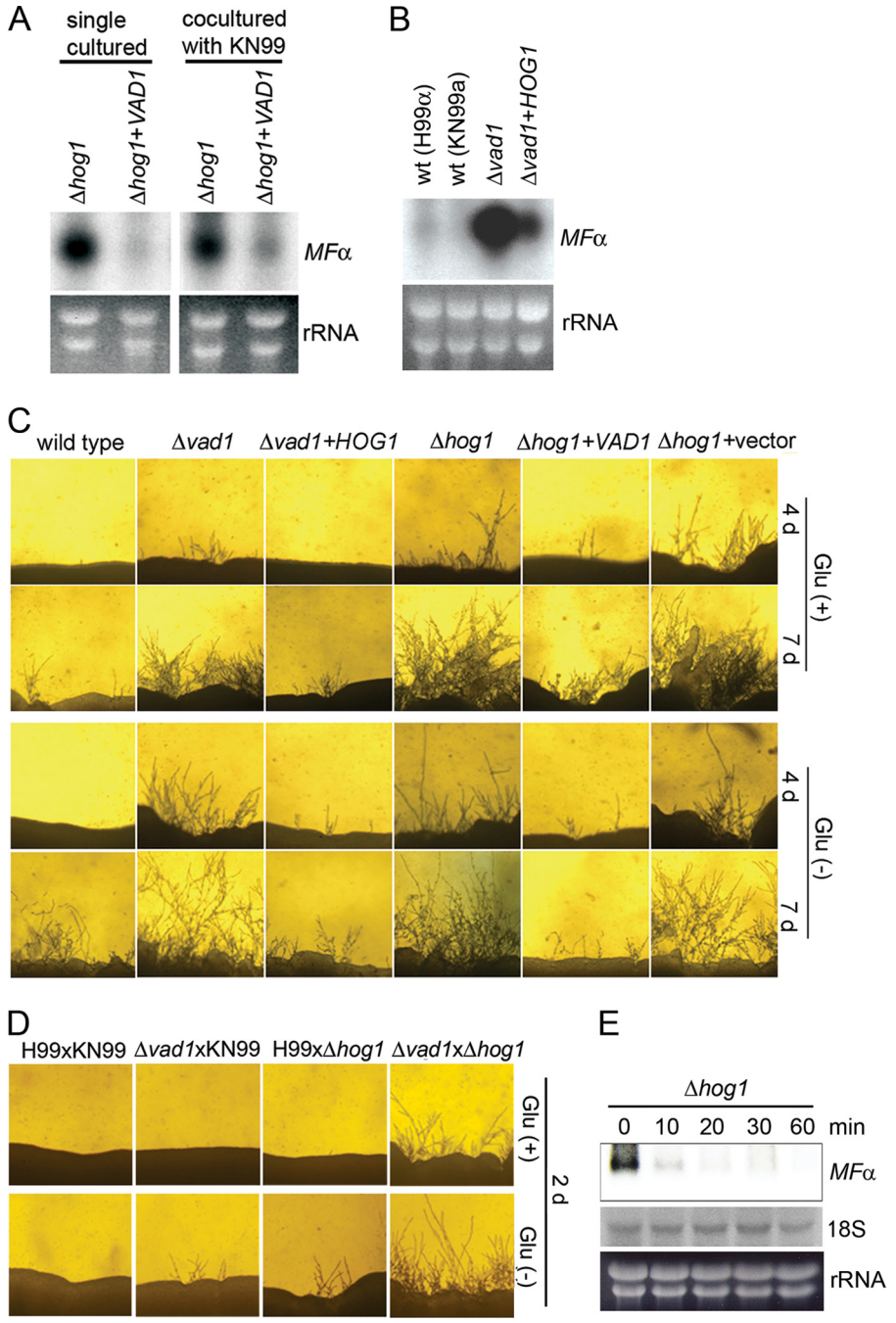

FIGURE 6. **Overexpression of either *VAD1* or *HOG1* restores wild type filamentation and *MFα* transcriptional levels in Δ*hog1* and Δ*vad1* mutant strains, respectively.** *A* and *B*, Northern blot analysis was performed with total RNA isolated from the indicated strains and hybridized with an ORF region from *MFα* genes. *C*, the indicated strains were co-cultured with KN99 on V8 medium and incubated at room temperature in the dark and observed at the indicated times. Representative edges of the mating patches were photographed at ×40 magnification. *D*, filamentation of Δ*hog1* and Δ*vad1* mutant cells co-cultured on V8 medium and incubated for 2 days at room temperature in the dark. *E*, degradation analysis of *MFα* was performed as described under "Experimental Procedures" using total RNA isolated from Δ*hog1* mutant strains.

ability to act as either enhancers or inhibitors of mRNA stability and translation efficiency (47). Because of an important role in both mating and virulence, we undertook further studies of *MFα* transcript regulation. Suggesting its role as an RNA transcriptional degradative factor, *MFα* mRNA accumulated in a *C. neoformans* Δ*vad1* mutant and was markedly reduced after *VAD1* overexpression. Perturbations of *MFα* transcriptional levels after *VAD1* gene dosing manipulation also correlated with MFα protein levels and filamentation, suggesting the central role of MFα in sexual development (15). This is similar to the role of Pub1p, an ELAV-like yeast RNA-binding protein with homology to TIA-1 (T-cell internal antigen 1)/TIAR (TIA-1-related protein), which binds to discrete subsets of cellular transcripts, regulating their expression at multiple levels (45). Indeed, Vad1 of *C. neoformans* shows homology to the Dhh1 RNA-binding protein of *S. cerevisiae*, a component of the cytoplasmic mRNA degradation complex, having 74% identity at the protein level (20, 40, 48, 49). Defects in components of the cytoplasmic mRNA deadenylase/decapping complex in *dhh1* mutants have been shown to accumulate partially degraded mRNAs associated with an increase in mRNA half-life (50). Interestingly, both the 5′- and 3′-UTRs of the *MFα* target transcript were required to potentiate *MFα1* degradation in the presence of *VAD1*. This may be due to binding of both regions to a Vad1-containing complex or a requirement of both regions for proper transcriptional secondary structure required for the formation of protein binding mRNA loops (51). In summary, regulation of mRNA turnover by Vad1 appears to be an important cellular strategy for reducing steady state levels of mating pheromone under conditions where mating is repressed.

An obvious question arises upon inspection of data from Fig. 1, *B* and *C*. Why do vegetative yeast cells synthesize ~17-fold more mating pheromone than is needed (as observed in the Δ*vad1* mutant) only to degrade the transcript to the low steady state levels of transcript observed in wild-type cells? This excessive synthesis would appear to be at great metabolic cost in vegetative cells and particularly difficult during periods of starvation. Indeed, in the present studies, maintenance of high levels of *MFα* transcription by overexpression resulted in reductions in pathogenic fitness exhibited by attenuated mortality after mouse inoculation (Fig. 4*E*). Such an apparent futile cycle of transcript synthesis and degradation has similarities to the classically described metabolic futile cycle (Fig. 7). Enzymatic futile cycles represent a recurring con-

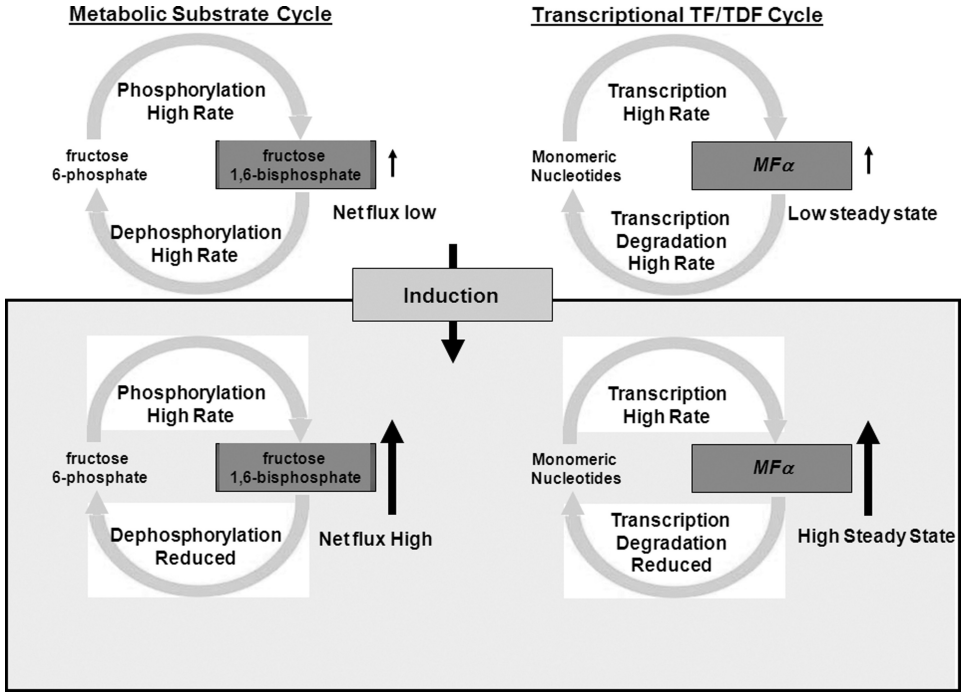

FIGURE 7. **Schematic of metabolic *versus* transcriptional regulatory cycles.** *TF*, transcription factor; *TDF*, transcription degradative factor.

trol motif in biological networks, appearing in a wide variety of processes from energy metabolism to signal transduction (52–54). In the example of muscle metabolism, fructose 6-phosphate and fructose 1,6-biphosphate undergo rapid interconversion at equal rates in the resting state, resulting in low levels of available fructose 1,6-bisphosphate (Fig. 7, *left*). However, the futile cycle retains high levels of phosphorylation/dephosphorylation enzyme activities that would be difficult to synthesize and assemble in a timely fashion. Upon muscle contraction, a rapid requirement for fructose 1,6-bisphosphonate is facilitated by the constitutive high levels of fructose 6-phosphate phosphorylation, requiring only small increases in rates of phosphorylation and small decreases in rates of dephosphorylation to produce large increases in fructose 1,6-bisphosphate for gluconeogenesis (55). In the same way, simultaneous high level production and degradation of *MFα* transcripts under vegetative conditions, although apparently wasteful from the energy standpoint, result in the retention of a high transcript synthetic capacity for rapid induction during periods conducive to mating (Fig. 7, *right*). This is particularly curious because yeasts such as *Cryptococcus* are thought to spend the vast majority of their time in the asexual state (7). In addition, repression of *MFα* under vegetative conditions appears to be important to a pathogen such as *C. neoformans* because high level expression of *MFα* results in reduced virulence in mice. In our experiments, transfer to pigeon guano mating medium resulted in rapid inhibition of *MFα* degradation and induction of successful mating within 6 h as described in this favored environmental medium of mating (3). Interestingly, maintenance of intact *MFα* degradation in a *VAD1* overexpressor strain after transfer to mating medium did not prevent mating; rather, overexpression increased the time to successful mating. This suggests that the metabolic cost of high level MFα synthesis during long periods of asexual growth may be justified by an ability to induce transcripts rapidly, similar to that exhibited by metabolic futile cycles. Rapid induction of mating may be important for fungi that are susceptible to physical forces disruptive of required intimate associations. In the case of *C. neoformans*, improving mating efficiency could help ensure sexual reproduction in an organism with low numbers of strains having opposite mating types (56, 57). In addition, this property of rapid induction may be important for the establishment of infection because spores created through mating have an approximately 100-fold increased infectious potential compared with the yeast form (5).

Interestingly, the transcriptional regulation of *MFα* by *VAD1* appeared by epistatic experiments to be parallel to that of the *HOG1* signal transduction pathway, although mutants of both genes showed similar mating phenotypes. In addition, *HOG1* signaling appeared to act though a process of transcript synthesis because degradation of *MFα* was intact even in Δ*hog1* mutants in our studies. Indeed, *HOG1* in the model yeast *S. cerevisiae* is thought to act on *MFα* through stress response elements in the promoter region of mating pheromones (58). This suggests that *HOG1* is involved in the opposing part of the transcriptional *MFα* cycle, regulating high level transcriptional synthesis of *MFα* similar to phosphorylation in the classic metabolic cycle. In our experiments, we did not find transcriptional induction upon a change from vegetative growth to one favoring mating that could be mediated by pathways such as *HOG1*. However, this lack of synthetic induction under the conditions tested should be interpreted with caution because we did not manipulate other environmental signals that could be environmentally important, such as osmolarity, which is known to affect *HOG1*-mediated signaling (59). Indeed, paradigms from more conventional substrate cycles suggest that both induction and degradation are important mechanisms of regulation during changes from repressive to inductive conditions.

REFERENCES

1. Morrow, C. A., and Fraser, J. A. (2009) *FEMS Yeast Res.* **9,** 161–177
2. Butler, G., Kenny, C., Fagan, A., Kurischko, C., Gaillardin, C., and Wolfe, K. H. (2004) *Proc. Natl. Acad. Sci. U.S.A.* **101,** 1632–1637
3. Nielsen, K., De Obaldia, A. L., and Heitman, J. (2007) *Eukaryotic Cell* **6,** 949–959
4. Xue, C., Tada, Y., Dong, X., and Heitman, J. (2007) *Cell Host Microbe* **1,** 263–273
5. Velagapudi, R., Hsueh, Y. P., Geunes-Boyer, S., Wright, J. R., and Heitman, J. (2009) *Infect. Immun.* **77,** 4345–4355
6. Giles, S. S., Dagenais, T. R., Botts, M. R., Keller, N. P., and Hull, C. M. (2009) *Infect. Immun.* **77,** 3491–3500
7. Casadevall, A., and Perfect, J. R. (1998) *Cryptococcus neoformans*, Ameri-

can Society for Microbiology Press, Washington, D. C.
8. Park, B. J., Wannemuehler, K. A., Marston, B. J., Govender, N., Pappas, P. G., and Chiller, T. M. (2009) *AIDS* **23,** 525–530
9. Kwon-Chung, K. J. (1975) *Mycologia* **67,** 1197–1200
10. Kwon-Chung, K. J. (1976) *Mycologia* **68,** 821–833
11. Davidson, R. C., Moore, T. D., Odom, A. R., and Heitman, J. (2000) *Mol. Microbiol.* **38,** 1017–1026
12. Shen, W. C., Davidson, R. C., Cox, G. M., and Heitman, J. (2002) *Eukaryotic Cell* **1,** 366–377
13. Fraser, J. A., Diezmann, S., Subaran, R. L., Allen, A., Lengeler, K. B., Dietrich, F. S., and Heitman, J. (2004) *PLoS Biol.* **2,** e384
14. Lengeler, K. B., Fox, D. S., Fraser, J. A., Allen, A., Forrester, K., Dietrich, F. S., and Heitman, J. (2002) *Eukaryotic Cell* **1,** 704–718
15. Nielsen, K., Heitman, J., and Jay, C. D. (2007) *Adv. Genet.* 143–173
16. Davidson, R. C., Nichols, C. B., Cox, G. M., Perfect, J. R., and Heitman, J. (2003) *Mol. Microbiol.* **49,** 469–485
17. Lengeler, K. B., Davidson, R. C., D'souza, C., Harashima, T., Shen, W. C., Wang, P., Pan, X., Waugh, M., and Heitman, J. (2000) *Microbiol. Mol. Biol. Rev.* **64,** 746–785
18. Wang, P., and Heitman, J. (1999) *Curr. Opin. Microbiol.* **2,** 358–362
19. Bahn, Y. S., Kojima, K., Cox, G. M., and Heitman, J. (2005) *Mol. Biol. Cell* **16,** 2285–2300
20. Panepinto, J., Liu, L., Ramos, J., Zhu, X., Valyi-Nagy, T., Eksi, S., Fu, J., Jaffe, H. A., Wickes, B., and Williamson, P. R. (2005) *J. Clin. Invest.* **115,** 632–641
21. Beckham, C., Hilliker, A., Cziko, A. M., Noueiry, A., Ramaswami, M., and Parker, R. (2008) *Mol. Biol. Cell* **19,** 984–993
22. Zhu, X., and Williamson, P. R. (2003) *Mol. Microbiol.* **50,** 1271–1281
23. Kwon-Chung, K. J. (1994) in *Molecular Biology of Pathogenic Fungi* (Maresca, B., and Kobayashi, G. S., eds) pp. 341–344, Telos Press, New York
24. Panepinto, J. C., Komperda, K. W., Hacham, M., Shin, S., Liu, X., and Williamson, P. R. (2005) *Infect. Immun.* **75,** 4769–4779
25. Liu, X., Hu, G., Panepinto, J., and Williamson, P. R. (2006) *Mol. Microbiol.* **61,** 1132–1146
26. Erickson, T., Liu, L., Gueyikian, A., Zhu, X., Gibbons, J., and Williamson, P. R. (2001) *Mol. Microbiol.* **42,** 1121–1131
27. Takizawa, P. A., and Vale, R. D. (2000) *Proc. Natl. Acad. Sci. U.S.A.* **97,** 5273–5278
28. Kraus, P. R., Boily, M. J., Giles, S. S., Stajich, J. E., Allen, A., Cox, G. M., Dietrich, F. S., Perfect, J. R., and Heitman, J. (2004) *Eukaryotic Cell* **3,** 1249–1260
29. Yoav, B., and Yosef, H. (1995) *J. R. Stat. Soc. Ser. B* **57,** 289–300
30. Bahn, Y. S., Hicks, J. K., Giles, S. S., Cox, G. M., and Heitman, J. (2004) *Eukaryotic Cell* **3,** 1476–1491
31. Hicks, J. K., D'Souza, C. A., Cox, G. M., and Heitman, J. (2004) *Eukaryotic Cell* **3,** 14–26
32. Hsueh, Y. P., Xue, C., and Heitman, J. (2007) *Mol. Biol. Cell* **18,** 3237–3249
33. Elion, E. A., and Warner, J. R. (1986) *Mol. Cell. Biol.* **6,** 2089–2097
34. Salas, S. D., Bennett, J. E., Kwon-Chung, K. J., Perfect, J. R., and Williamson, P. R. (1996) *J. Exp. Med.* **184,** 377–386
35. Hu, G., Hacham, M., Waterman, S. R., Panepinto, J., Shin, S., Liu, X., Gibbons, J., Valyi-Nagy, T., Obara, K., Jaffe, H. A., Ohsumi, Y., and Williamson, P. R. (2008) *J. Clin. Invest.* **118,** 1186–1197
36. Moore, T. D., and Edman, J. C. (1993) *Mol. Cell. Biol.* **13,** 1962–1970
37. D'Souza, C. A., Alspaugh, J. A., Yue, C., Harashima, T., Cox, G. M., Perfect, J. R., and Heitman, J. (2001) *Mol. Cell. Biol.* **21,** 3179–3191
38. Wichroski, M. J., Robb, G. B., and Rana, T. M. (2006) *PLoS Pathog.* **2,** e41
39. Grigull, J., Mnaimneh, S., Pootoolal, J., Robinson, M. D., and Hughes, T. R. (2004) *Mol. Cell. Biol.* **24,** 5534–5547
40. Coller, J. M., Tucker, M., Sheth, U., Valencia-Sanchez, M. A., and Parker, R. (2001) *RNA* **7,** 1717–1727
41. Goeres, D. C., Van Norman, J. M., Zhang, W., Fauver, N. A., Spencer, M. L., and Sieburth, L. E. (2007) *Plant Cell* **19,** 1549–1564
42. Kebaara, B., Nazarenus, T., Taylor, R., Forch, A., and Atkin, A. L. (2003) *Nucleic Acids Res.* **31,** 3157–3165
43. Sakuno, T., Araki, Y., Ohya, Y., Kofuji, S., Takahashi, S., Hoshino, S., and Katada, T. (2004) *J. Biochem.* **136,** 805–812
44. Ingelfinger, D., Arndt-Jovin, D. J., Lührmann, R., and Achsel, T. (2002) *RNA* **8,** 1489–1501
45. Duttagupta, R., Tian, B., Wilusz, C. J., Khounh, D. T., Soteropoulos, P., Ouyang, M., Dougherty, J. P., and Peltz, S. W. (2005) *Mol. Cell. Biol.* **25,** 5499–5513
46. del Poeta, M., Toffaletti, D. L., Rude, T. H., Sparks, S. D., Heitman, J., and Perfect, J. R. (1999) *Infect. Immun.* **67,** 1812–1820
47. Wilusz, C. J., Wormington, M., and Peltz, S. W. (2001) *Nat. Rev. Mol. Cell Biol.* **2,** 237–246
48. Hata, H., Mitsui, H., Liu, H., Bai, Y., Denis, C. L., Shimizu, Y., and Sakai, A. (1998) *Genetics* **148,** 571–579
49. van Dijk, E., Cougot, N., Meyer, S., Babajko, S., Wahle, E., and Séraphin, B. (2002) *EMBO J.* **21,** 6915–6924
50. Fischer, N., and Weis, K. (2002) *EMBO J.* **21,** 2788–2797
51. Mao, H., White, S. A., and Williamson, J. R. (1999) *Nat. Struct. Mol. Biol.* **6,** 1139–1147
52. Horsthemke, W., and Lefever, R. (1977) *Phys. Lett.* **64A,** 19–21
53. Pomerening, J. R., Sontag, E. D., and Ferrell, J. E., Jr. (2003) *Nat. Cell Biol.* **5,** 346–351
54. Hasty, J., Pradines, J., Dolnik, M., and Collins, J. J. (2000) *Proc. Natl. Acad. Sci. U.S.A.* **97,** 2075–2080
55. Suh, S. H., Paik, I. Y., and Jacobs, K. (2007) *Mol. Cells* **23,** 272–279
56. Lin, X., Hull, C. M., and Heitman, J. (2005) *Nature* **434,** 1017–1021
57. Fraser, J. A., Giles, S. S., Wenink, E. C., Geunes-Boyer, S. G., Wright, J. R., Diezmann, S., Allen, A., Stajich, J. E., Dietrich, F. S., Perfect, J. R., and Heitman, J. (2005) *Nature* **437,** 1360–1364
58. Sunnarborg, S. W., Miller, S. P., Unnikrishnan, I., and LaPorte, D. C. (2001) *Yeast* **18,** 1505–1514
59. Alonso-Monge, R., Navarro-García, F., Román, E., Negredo, A. I., Eisman, B., Nombela, C., and Pla, J. (2003) *Eukaryotic Cell* **2,** 351–361